J Mater Sci: Mater Electron (2021) 32:9998–10007

Investigations on Al_2O_3 dispersed PEO/PVP based Na^+ ion conducting blend polymer electrolytes

S. Shenbagavalli[1,2], M. Muthuvinayagam[1,*], S. Jayanthi[3], and M. S. Revathy[1]

[1] *Department of Physics, School of Advanced Sciences, Kalasalingam Academy of Research and Education, Tamil Nadu, Krishnankoil-626126, Virudhunagar, India*

[2] *Multifunctional Materials Laboratory, International Research Centre, Kalasalingam Academy of Research and Education, Tamil Nadu, Krishnankoil-626126, Virudhunagar, India*

[3] *Department of Physics, The Standard Fireworks Rajaratnam College for Women (Autonomous), Tamil Nadu, Sivakasi-626123 Virudhunagar, India*

Received: 1 November 2020
Accepted: 1 March 2021
Published online: 30 March 2021

ABSTRACT

In this current study, Na^+ ion conducting solid blend polymer electrolytes (NCSBPEs) based on polyethylene oxide (PEO) / polyvinyl pyrrolidine (PVP) / sodium nitrate ($NaNO_3$) with the addition of different wt.% aluminum oxide (Al_2O_3) as filler were prepared using solution casting technique. The prepared solid blend polymer electrolytes are subjected to X-ray diffraction (XRD), Fourier transforms infrared (FTIR), and AC-impedance techniques. The complexation has been studied using X-ray diffraction (XRD) and Fourier transform infrared spectroscopy (FT-IR) measurements. AC-impedance spectroscopy has been used to analyze the ionic conductivity of the solid blend polymer electrolytes. The higher ionic conductivity (σ) $\sim 10^{-7}$ S/cm^{-1} is obtained for PEO: PVP: $NaNO_3$ film and it was enhanced to $\sim 10^{-5}$ S/cm^{-1} with the addition of Al_2O_3 filler at the ambient temperature. The dielectric and tan δ values were also calculated using the impedance analysis. In LSV (linear sweep voltammetry) studies, a broad electrochemical stability window was observed for polymer electrolytes besides CV (cyclic voltammetry) studies confirm the electrochemical behavior of the electrolytes.

1 Introduction

Nowadays, Solid Polymer Electrolytes (SPEs) are one of the greatest reliable materials for the production of powerful batteries, supercapacitors, and fuel cells. Solid polymer electrolytes are used as a key component of modern solid-state technology devices. Polymer electrolytes are known as ionic conductors which are formed by salts with polymers of high-atomic weight polymers. The main advantages of polymer electrolytes are their mechanical properties, good electrochemical precision, adaptability, ease of

Address correspondence to E-mail: mmuthuvinayagam@gmail.com

https://doi.org/10.1007/s10854-021-05658-3

different sizes of thin film, and the ability to design precise electrode/electrolyte contacts for electrochemical devices [1, 2]. However, in potential battery advances, the overwhelming cost, lack of availability, environmental impact, and concern for lithium materials have hindered their remote usage [3]. Alternate energy storage devices are important instead of lithium battery. Due to their environmental-friendly, lower cost, low toxic, and earth-abundant materials, sodium (Na) ion batteries (SIBs) have received a lot of attention. Polymer compounds contain the physical structure of two or more structurally different homopolymers or copolymers, and they interact without covalent bonding throughout secondary forces. Polymers used for blending are soluble in water which is a significant property of film making [4].

The SPEs film based on the use of appropriate polymer blend as hosts that are treated with appropriate types of sodium salt has been widely studied to develop all sodium-ion cells in solid states due to several advantages in terms of high ambient conductivity, flexibility, good compatibility with chemicals, good contact with electrodes/electrolytes, improved mechanical properties and ease of device fabrication [5].

Poly (ethylene oxide) (PEO) is an amorphous, crystalline, micro-structured semi-crystalline polymer. Different forms of reactive metal salts such as Li, Na, and Mg may be formed into complex PEOs [5, 6]. In the beginning, the presence of crystalline phases helped to transport ions in PEO, and ions were assumed to be transported with PEO. The simultaneous operation in PEO activation of amorphous phases can nevertheless be established quickly [7]. Poly (ethylene oxide) is the polymer most used in solid electrolyte formation [8]. Significant ionic conductivity of PEO is diminished by increasing crystallization due to transportation in the amorphous region [9]. Poly (vinylpyrrolidone) (PVP), due to its special properties, is a promising source for the preparation of PEO polymer composites. In the first place, PVP is an amorphous polymer with a high-temperature glass transition (T_g) [10] because of its rigid pyrrolidone portion, which allows ionic motion faster than other semi-crystalline polymers. Secondly, the occurrence in the PVP side chains of a carbonyl group (C = O) promotes the complex formation of several inorganic salts [11]. Most widely used host polymers for the development of sodium ion-conducting SPEs films include PEO, poly (methyl methacrylate) (PMMA), poly (vinylidene fluoride) (PVDF) and poly (vinyl alcohol) (PVA) which can be solved with various sodium salts such as $NaClO_4$, $NaPF_6$, $NaBF_4$, NaTFSI, Na_2SO_4, NaFSI, NaYF4, NaI and $NaCF_3SO_3$ to synthesize the [12–23] SPEs. In the current study, sodium nitrate ($NaNO_3$) is selected as the Na source for doping PEO/PVP polymer blend. $NaNO_3$ can be handled under ambient conditions and systems based on $NaNO_3$ dopant have already been reported [24].

Therefore, significant effort was made to increase the solid polymer electrolyte's ionic conductivity. Incorporating plasticizers into polymer electrolyte will improve the performance. This results in high ambient conductivity though it promotes the degradation of the mechanical properties of the electrolyte.

Dispersion of inert, ceramic oxide fillers like TiO_2, Al_2O_3, SiO_2, ZrO_2, $BaTiO_3$, $Sb2O_3$, Na_2SiO_3, and SnO_2 [25–29] is an interesting approach to further improve the electrochemical properties of the SPE films. The addition of the fillers is expected to modify the degree of the crystalline nature and tailor the local structure, morphology, and flexibility of the polymer backbone and the ion mobility through the SPEs films [30]. This improves the amorphous nature of the host polymer by reducing the recrystallization rate and enhances the interfacial stability and ionic conductivity [13].

It was proposed in many kinds of literature that improving the conductivity by increasing the defined surface area of filler grain would increase. When the filler grain is used in maximum range, a considerable increase in the ability of conductivity can be achieved as it is about the nature of the Lewis acid–base groups on the grain surface [31]. The addition of Al_2O_3 as an active filler material to the polymer blend leads to surface functionality by forming O-OH groups on the specimen surfaces which in turn leads to hydrogen bonding with migrating ionic species to the improved ionic conductivity of SPEs films.

The combined effect of PEO/PVP/$NaNO_3$ based solid blend polymer electrolytes (NCSBPEs) along with Al_2O_3 ceramic filler will be of great interest to study. Various methods such as FTIR, AC impedance technique, cyclic voltammetry (CV), and linear sweep voltammetry technique (LSV) are used to characterize the prepared electrolytes.

2 Materials and methods

2.1 Materials

The polymers PEO (Mw of 5×10^6 g/mol) and PVP (Mw = 90,000 g/mol) were purchased from SD Fine Chem Ltd., India. Sodium nitrate ($NaNO_3$) (Merck India) is used as salt. Al_2O_3 was purchased from SD fine chem Ltd. During this experiment, double distilled water is used as the solvent.

2.2 Synthesis of Polymer electrolytes

The solid blend polymer electrolytes (SBPEs) consisting of PEO / PVP / $NaNO_3$ and Al_2O_3 were prepared by the solution casting technique using double-distilled water (D.D water) as a solvent. The precursor content stoichiometric amounts are 67wt.% PEO / 27wt.% PVP and 6wt% $NaNO_3$ which have been dissolved separately by distilled water and they were continuously agitated at 40° C for six hours to form transparent solutions. The above described transparent PEO / PVP / $NaNO_3$ solutions are mixed with stirring to get a homogenous solution. Then, the fillers, Al_2O_3 are applied to the above solution with varying concentrations from 1 wt.% to 5 wt.% (in steps of 1 wt.%) and well stirred at room temperature. The obtained homogeneous solution PEO / PVP / $NaNO_3$ / Al_2O_3 was then poured into polypropylene dishes and allowed to dry gradually for 4 days at room temperature. The polymer film obtained from the blend is peeled off from dishes and placed inside a desiccator for further characterizations. Figure 1 shows the preparation method of polymer electrolytes.

2.3 Characterization techniques

2.3.1 XRD spectroscopy

To confirm the structural identification, an X-Ray diffraction pattern has taken for all the blend polymers using Bruker made X-Ray diffractometer with a wavelength of 1.540 A° at 5° per minute scanning rate from 10° to 60°.

2.3.2 FTIR spectroscopy

FTIR transmittance spectra of the films are recorded using SHIMADZU IR Tracer 100 spectrometer in the wavenumber range between 4000 cm^{-1} and 400 cm^{-1}.

2.3.3 AC impedance spectroscopy

HIOKI 3532–50 LCR Hi-tester within the frequency region from 42 Hz to 1 MHz is used to find the electrical properties of solid polymer electrolytes.

2.3.4 Electrochemical potential window

The electrochemical properties of the electrolytes are analyzed by CV and LSV analysis using CH-Instrument Model 6008e.

3 Result and discussion

3.1 XRD analysis

Figure 2 shows the XRD pattern of PEO / PVP/ $NaNO_3$ incorporated with nanofiller Al_2O_3 with different wt.% ratios (a) (67:27:6:1), (b) (67:27:6:2), (c) (67:27:6:3), (d) (67:27:6:4) and (e) (67:27:6:5). While increasing higher concentration of Al_2O_3, peak intensity decreases up to 4wt.% of Al_2O_3 concentration then peak intensity increases. Thus 4wt.% of Al_2O_3 doped system possess higher amorphous nature, leading to the maximum ionic conductivity than the other polymer electrolytes. The peaks at 2θ = 29.0, 30.9, 38.2, and 44.2 in the diffraction pattern shows that Al_2O_3 is dispersed in the electrolytes [32]. This finding confirms the occurrence of Lewis acid–base interactions and thus creates the ion-filler complex. The amorphous nature of the blend is improved by the intermolecular interaction between polymer blend in C–O–C group of PEO and/or C = O group of PVP of a polymer blend with salt [33]. It would be more useful to reduce the continuous chain of the polymer and to close the packing system. As a result, the crystallinity decreases up to the concentration of 4 wt.% Al_2O_3. The peaks due to Al_2O_3 are found to be absent in polymer electrolytes that reveal the complete dissociation of filler. With the further addition of filler up to 5wt.% Al_2O_3, the intensity of the peak is increased (Fig. 2 e) due to incomplete dissociation of filler in the polymer matrix.

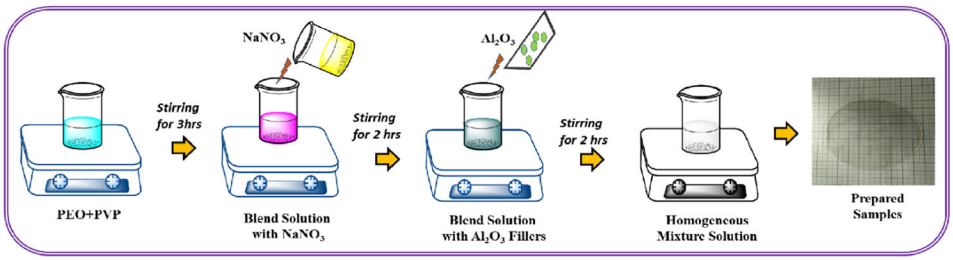

Fig. 1 Schematic diagram of solution casting technique

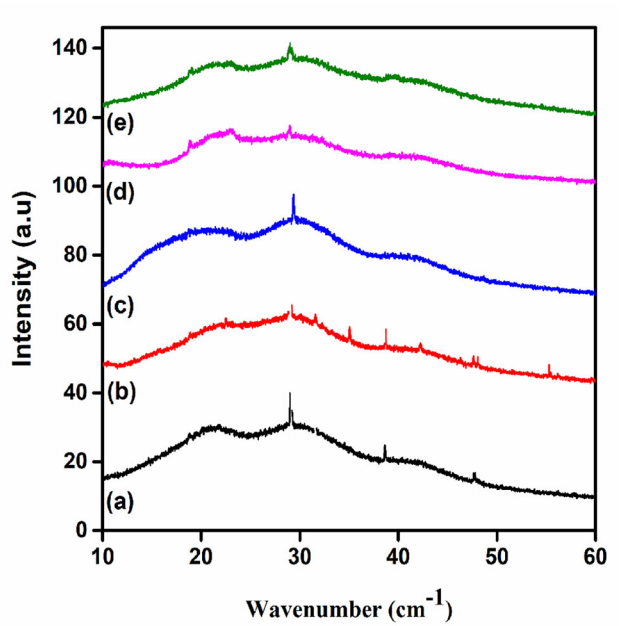

Fig. 2 XRD analysis of PEO/PVP/$NaNO_3$/Al_2O_3 blend Polymer Electrolytes

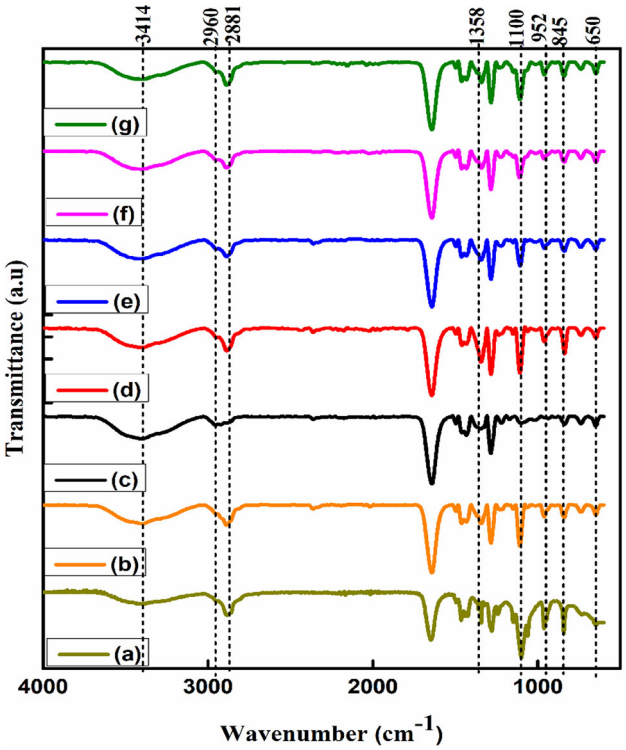

Fig. 3 FTIR spectra of PEO/PVP/$NaNO_3$/Al_2O_3 blend Polymer Electrolytes (4000 cm^{-1}–500 cm^{-1}) and (a) PEO/ PVP, (b) PEO/ PVP/$NaNO_3$, and PEO/PVP/$NaNO_3$/ different wt.% Al_2O_3 system for (c) x = 1, (d) x = 2, (e) x = 3, (f) x = 4, (g) x = 5

3.2 FTIR studies

Figure 3a–g displays the PEO/PVP blend, PEO/PVP blend with 6 wt.% $NaNO_3$, and the PEO/PVP/$NaNO_3$ with different wt.% of Al_2O_3 respectively. The FTIR spectroscopy data shows the complexity among the individual components of the solid blend polymer electrolytes system. The absorption of strong peaks among 2881 cm^{-1} and 2960 cm^{-1} is resembled (C-H) stretching vibrations in the CH_2 group of PEO as shown in the spectrum. The band placed at 842 cm^{-1} is assigned to the PVP rocking mode of CH_2, with the PEO being associated with a minor contribution from the stretching mode C–O. The 952 cm^{-1} band is related to the PEO vibration stretch mode of C–O [24]. The IR mode of anion (NO_3^-) characteristics of the salt polymer matrix are located at 650, and 1350 cm^{-1} [34]. The peak of intensity is reduced as shown in Fig. 3b–g, as $NaNO_3$ salt is present [12]. The peak at 1100 cm^{-1} is associated with the C–O–C stretching mode in the pure PEO. In Fig. 2b–g, shows that the associated peak is increased and its intensity is decreased. The Na + ions of $NaNO_3$ coordination with the ether oxygen of PEO result in the observed reduction of peak intensity [35] and indicate that $NaNO_3$ the complex with the PEO/ PVP blend. In Fig. 3e–g are retained the typical absorption peaks of the PEO and it demonstrates that the structure of the PEO system does not be affected by the inclusion of Al_2O_3 [32, 36, 37]. Thus, this spectrum confirms the blending of polymers, salt, and ceramic filler.

3.3 AC impedance spectroscopy

3.3.1 Cole–Cole plot

The diagram indicates the PEO/PVP /$NaNO_3$ / Al_2O_3 solid blend polymer electrolytes at different compositions of Al_2O_3. With an inclined spike, the depressed semi-circle shows the free moment of ions, created by Non-Debye nature. The depressed semi-circle and incline spike obtained corresponds to the capacitation series associated with the parallel capacitor combination (C_p) and the bulk resistance (R_b) [38]. The bulk resistance (R_b) is measured at low-frequency from the edge of impedance which touches the real axis (Z′) [39–41].

The obtained data were also fitted using Z-View software to calculate the bulk resistance. Using the following relationship, the ionic conductivity of the prepared samples is measured.

$$\sigma = l/AR_b \quad (1)$$

where l is the sample size, A is the electrode area used (silver electrode), and R_b is the bulk resistance.

From this Table 1, the value of conductivity increases from $\sim 10^{-7}$ S cm^{-1} observed for 0 wt.% Al_2O_3 to a maximum of $\sim 10^{-5}$ S cm^{-1} at ambient temperature for 4wt.% of filler added system in Fig. 4. Also, the presence of the filler improves the salt dissociation process and increases the number of charge carriers. The addition of Al_2O_3 (i.e. 5wt.% of filler), reduces ionic conductivity due to the more abundant alumina blocking effect that improves the immobilization of the polymer chains, which leads to a lower ionic conductivity [39].

Table 1 Values of ionic conductivity of Al_2O_3 added PEO/PVP/$NaNO_3$ systems

Concentrations of Al_2O_3 (wt.%)	Ionic Conductivity (S cm^{-1})
1	2.455×10^{-6}
2	1.784×10^{-6}
3	3.223×10^{-6}
4	$\mathbf{1.869 \times 10^{-5}}$
5	3.873×10^{-6}

Bold content (ionic conductivity) denotes room temperature conductivity

3.3.2 Conduction spectra

In the conductance spectra, there are three distinct regions: low-frequency region, mid-frequency plateau region, and high-frequency dispersion region as shown in Fig. 5. The plateau region has a relation of long-range of low-frequency hopping ions [42]. The dc conductivity can be measured by extending the curve along the y (log σ) axis towards the lower frequency. There is an increase in conductivity at high frequencies, due to the simultaneous forward and backward motion of the ions, thus increasing the mobility of the alleged ions due to the universal power-law behavior of the polymer electrolytes.

3.3.3 Dielectric spectra analysis

The dielectric relaxation behavior of the polymer electrolytes gives valuable insights into the phenomenon of ion transport [43]. Figure 6a and b giving a variance in dielectric permittivity and dielectric constant at different wt.% of Al_2O_3 for $NaNO_3$ complexes PEO/PVP blend polymer matrix. The lower frequency region creates a high dielectric constant through the accumulation of charges at the electrode and electrolyte interface, which induces space charges and charge polarization in that region [44–52]. The dielectric permittivity at high frequencies is

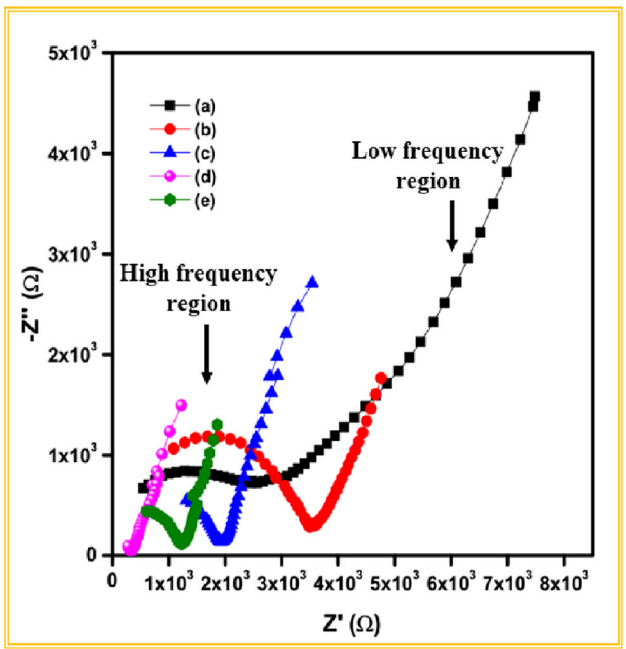

Fig. 4 AC impedance plot of PEO/PVP/$NaNO_3$/Al_2O_3 system at room temperature

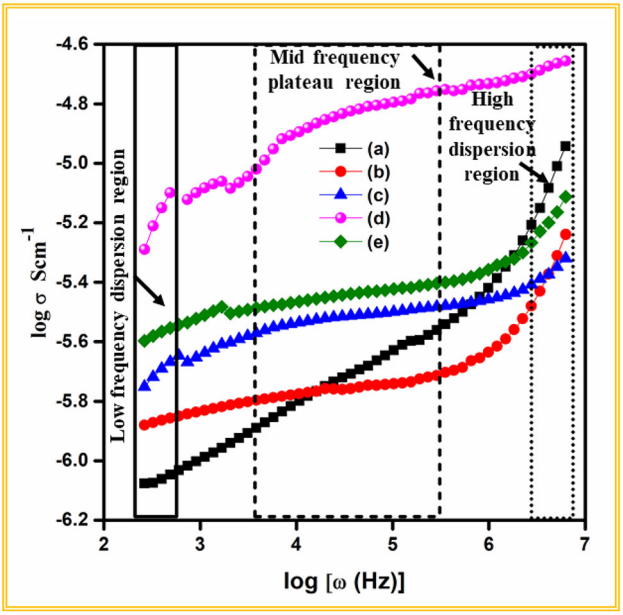

Fig. 5 Conductance Spectra of PEO/PVP/$NaNO_3$/Al_2O_3 system at room temperature

completely independent of the frequency. This may be attributed to the frequent reversal of the electric field located in the direction of the field of charging carriers.

3.3.4 *Complex modulus study (argand plot)*

Figure 7 shows that the complex modulus spectrum (M′ versus M″) for various wt.% of Al_2O_3 added PEO/PVP/$NaNO_3$ blend polymer electrolytes at room temperature. The ionic conductivity and relaxation of the polymer electrolytes contribute to a semi-circular arc of the Argand plot [53]. The radius of the semicircle arcs is decreasing as the filler content increase in the polymer electrolyte. A decrease of the semicircle arc by radius implies a decrease in the ion relaxation time in the polymer electrolytes. A higher conducting sample in the Argand plot has a lower semicircle arc and has a low relaxation time.

3.3.5 *Tangent spectra analysis*

The loss tangent (tan δ) is the loss factor ratio of the dielectric constant, which also implies the calculation of the energy loss ratio to the energy stored on a periodic electric field. The tan δ is defined according to the following expression,

$$\tan \delta = \varepsilon'/\varepsilon'' \tag{2}$$

The relaxation time, τ of each sample was calculated by equation,

$$\omega \tau = 1 \tag{3}$$

$$\omega = 2\pi f \tag{4}$$

Here, τ is the relaxation time, ω is the angular velocity with ω = 2πf, and f is the frequency value corresponding to maximum tan δ in Hz.

The peak maxima of tan δ shifts towards the higher frequency range with the increase of Al_2O_3 filler

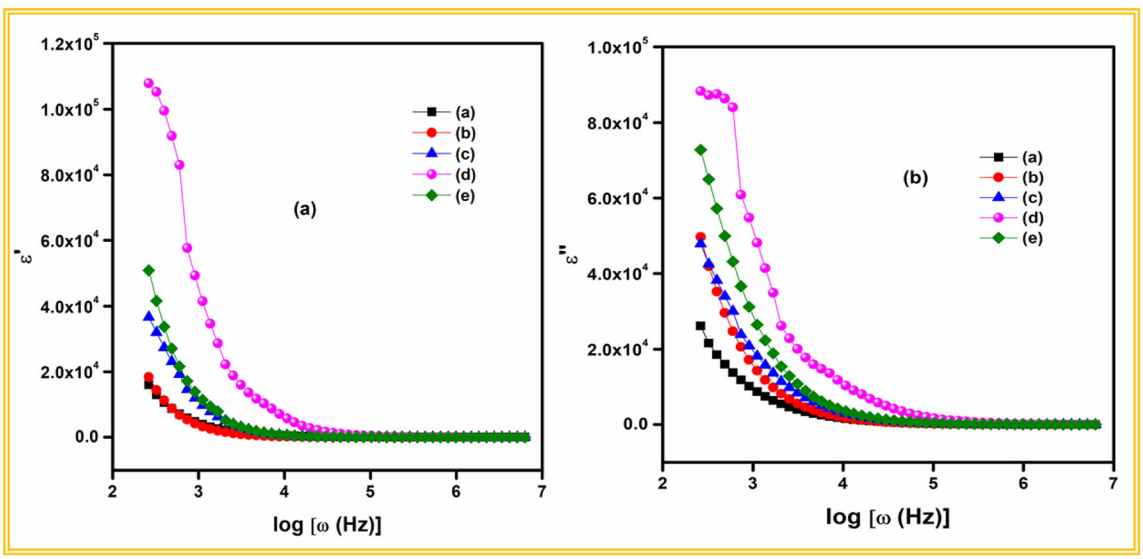

Fig. 6 Variation of the **a** dielectric permittivity versus log ω **b** dielectric loss versus log ω for PEO/PVP/$NaNO_3$/Al_2O_3 system at room temperature

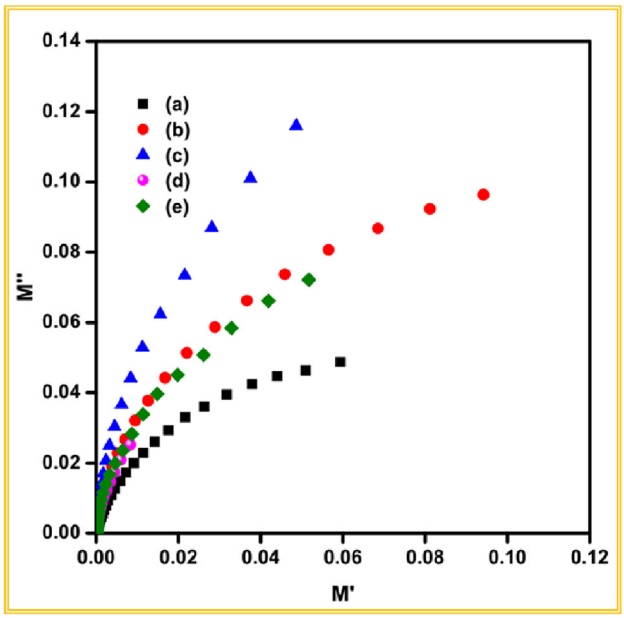

Fig. 7 Complex modules spectra of PEO/PVP/$NaNO_3$/Al_2O_3 system at room temperature

concentration. In the meantime, when the peak is shifted to a higher frequency, relaxation time is decreased. The calculated values of relaxation time for PEO / PVP / $NaNO_3$ system at different wt.% of Al_2O_3 are tabulated in Table 2. From this table, it is observed that the relaxation occurs at the higher frequency side and no relaxation occurs at the lower frequency side. As the concentration of Al_2O_3 increases, the values of relaxation time decrease and are found to consistent with ionic conductivity and Argand plot. Based on the report relaxation time value, the relaxation time is inversely proportional to the ionic conductivity of solid blend polymer electrolytes (Fig. 8).

Table 2 Values of relaxation time for Al_2O_3 added PEO/PVP/$NaNO_3$ system at various concentration

Concentrations of Al_2O_3 (wt.%)	Relaxation time τ (sec)
1	2.034×10^{-5}
2	2.224×10^{-5}
3	6.113×10^{-6}
4	$\mathbf{1.415 \times 10^{-6}}$
5	7.559×10^{-6}

Bold content (ionic conductivity) denotes room temperature conductivity

3.4 Cyclic voltammetry

Cyclic Voltammetry (CV) curves for different scan rates are shown in Fig. 9. The reproducible and clarity of the cyclic voltammetry curves will measure the sample purity and electrochemical stability [54]. Cyclic Voltammetry (CV) stability window of the solid polymer electrolytes (SPEs) sample from the curve is considered to be within -5 V to 5volt range. From this graph, polymer electrolyte is analysed by several scan rate (5 mVs^{-1}, 10 mVs^{-1}, 25 mVs^{-1}, 50 mVs^{-1}, 75 mVs^{-1}, 100 mVs^{-1}). When the scan rate increases, the area of the curve decreases. Area values following different scan rates for each sample are summarized in Table 3. The scan rate versus area is plotted in Fig. 10. The electrolyte provides easy ion mobility that provides only electrode related oxidation and reduction peaks, which establishes proper interface compatibility and ionic motion in the prepared electrolyte membrane [55].

3.5 Linear sweep voltammetry

The electrochemical stability window for the solid blend polymer electrolytes was calculated using linear sweep Voltammetry (LSV). LSV measurements of the higher ionic conductivity electrolytes were performed using silver electrodes at 4wt.% of Al_2O_3. The potential range was swept from 0 to 5 V until a large

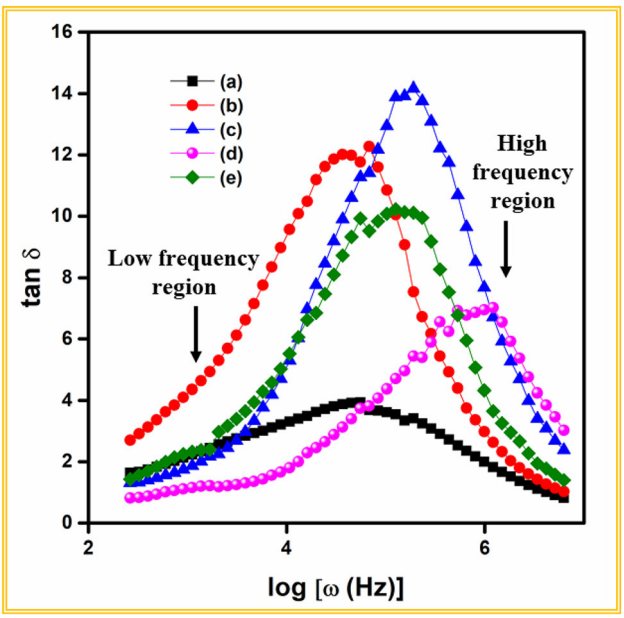

Fig. 8 Loss tangent spectra of PEO/PVP/$NaNO_3$/Al_2O_3 system at room temperature

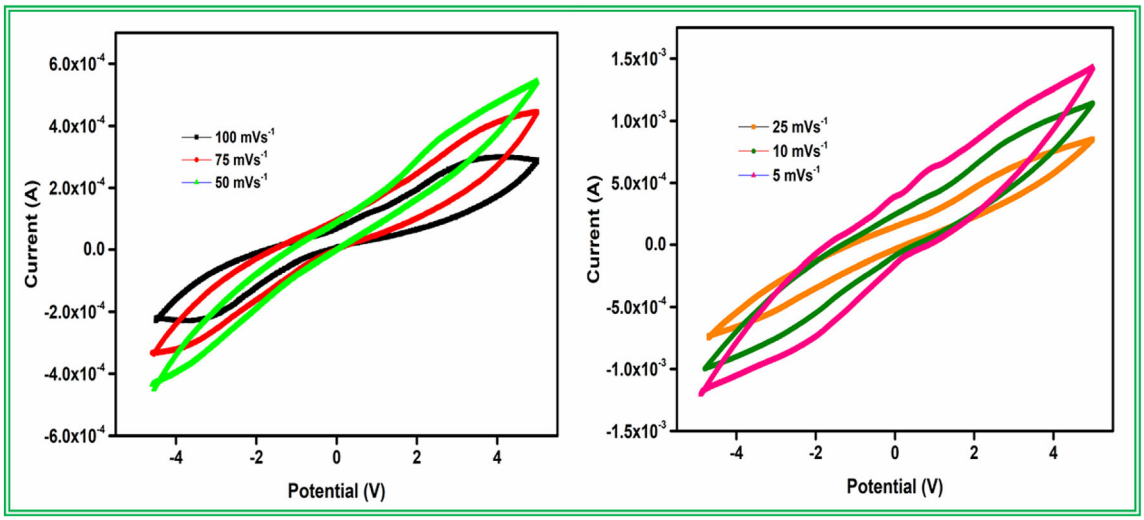

Fig. 9 CV curve of PEO/PVP/$NaNO_3$/ 4wt.%Al_2O_3 system at different scan rate of (5 mVs^{-1}, 10 mVs^{-1}, 25 mVs^{-1},50 mVs^{-1}, 75 mVs^{-1},100 mVs^{-1})

Table 3 Scan rate verses Area

Scan rate (mV s^{-1})	Area
5	4.669×10^{-2}
10	3.060×10^{-2}
25	1.784×10^{-2}
50	1.150×10^{-2}
75	9.469×10^{-4}
100	9.696×10^{-4}

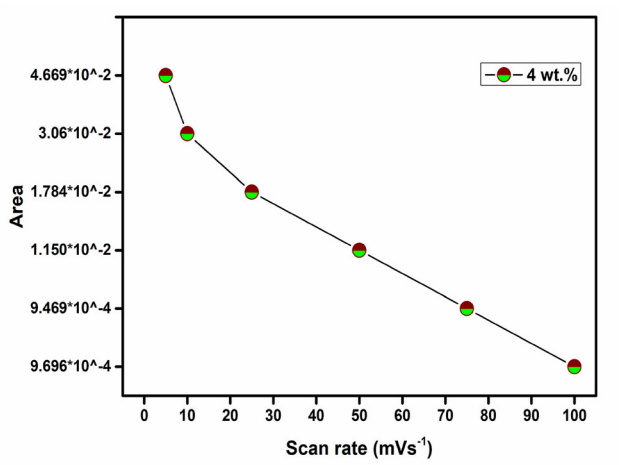

Fig. 10 Scan rate verses Area

current was obtained. To obtain the value of the decompose voltage, a straight line was drawn concerning the constant current and sharp current increase. The polymer electrolyte decomposition voltage is calculated as the current which flows through the cell [56]. The electrochemical stability window of PEO/PVP/$NaNO_3$/Al_2O_3 is ~ 2.69 V as shown in Fig. 11. The small current may be due to an alternation of the surface of the silver electrode [57]. When the cut-off voltage is reached the current started to increase, indicating that the electrolyte decay process had taken place [58, 59]. The cut-off voltage (the starting decomposition voltage) is greater for the SPE sample containing PEO/PVP/$NaNO_3$/ 4wt.%Al_2O_3.

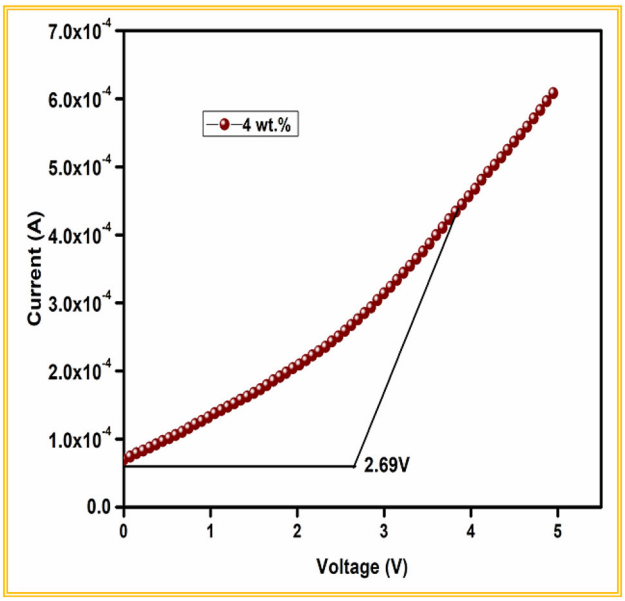

Fig. 11 LSV curve of PEO /PVP/$NaNO_3$/ 4wt.% Al_2O_3 system

4 Conclusion

The new PEO/PVP/$NaNO_3$ solid blend polymer electrolytes were successfully prepared using Al_2O_3 as filler with solution casting technique. The increase in the amorphous nature of the polymer electrolytes due to the addition of filler concentration is confirmed by XRD analysis. The FTIR analysis confirms the complexation between polymers, salt, and filler. For 4 wt.% Al_2O_3, the maximum ionic conductivity of $\sim 10^{-5}$ S cm^{-1} is observed at room temperature. An increase in the dielectric constant is found by increasing the filler concentrations. The peaks in the loss tangent plot shift to a higher frequency region by increasing the filler concentration and this results in to decrease in relaxation time. Cyclic Voltammetry (CV) studies confirm the electrochemical property of the solid polymer electrolytes (SPEs) and LSV studies provide the electrochemical stability window (2.69-volt) of the polymer membranes. Thus, the prepared polymer electrolytes are suitable for energy storage devices.

References

1. S. Ramesh, G.B. Teh, R.F. Louh, Y.K. Hou, P.Y. Sin, L.J. Yi, Sadhana - Acad. Proc. Eng. Sci. **35**, 87 (2010)
2. J.S. Kumar, M.J. Reddy, U.V.S. Rao, J. Mater. Sci. **41**, 6171 (2006)
3. A. Karmakar, A. Ghosh, Curr. Appl. Phys. **12**, 539 (2012)
4. S.A. Jones, G.P. Martin, P.G. Royall, M.B. Brown, J. Appl. Polym. Sci. **98**, 2290 (2005)
5. K.K. Kumar, Y. Pavani, M. Ravi, S. Bhavani, A.K. Sharma, V.V.R.N. Rao, A.I.P. Conf, Proc. **1391**, 641 (2011)
6. A.B. Puthirath, B. John, C. Gouri, S. Jayalekshmi, Ionics (Kiel). **21**, 2185 (2015)
7. K.M. Anilkumar, B. Jinisha, M. Manoj, S. Jayalekshmi, Eur. Polym. J. **89**, 249 (2017)
8. V. Thangadurai, W. Weppner, Ionics **8**, 281 (2002)
9. J.Y. Song, Y.Y. Wang, C.C. Wan, J. Power Sources **77**, 183 (1999)
10. H. Feng, Z. Feng, L. Shen, Polymer (Guildf). **34**, 2516 (1993)
11. P. Hu, J. Zhao, T. Wang, C. Shang, J. Zhang, B. Qin, Z. Liu, J. Xiong, G. Cui, Electrochem. Commun. **61**, 32 (2015)
12. T. Sreekanth, M.J. Reddy, S. Ramalingaiah, and UV Subba Rao. J. Power Sources **79**, 105 (1999)
13. Y.L. Ni'Mah, M.Y. Cheng, J.H. Cheng, J. Rick, B.J. Hwang, J. Power Sources **278**, 375 (2015)
14. A.M. Stephan, K.S. Nahm, Polymer (Guildf). **47**, 5952 (2006)
15. S.R. Mohapatra, A.K. Thakur, R.N.P. Choudhary, Ionics (Kiel). **14**, 255 (2008)
16. M. Patel, K.G. Chandrappa, A.J. Bhattacharyya, Solid State Ionics **181**, 844 (2010)
17. A. Boschin, P. Johansson, Electrochim. Acta **211**, 1006 (2016)
18. Y. Xue, D.J. Quesnel, RSC Adv. **6**, 7504 (2016)
19. S.S. Rao, M.J. Reddy, E.L. Narsaiah, and UV Subba Rao. Mater. Sci. Eng. B **33**, 173 (1995)
20. S.K. Tripathi, A. Gupta, M. Kumari, Bull. Mater. Sci. **35**, 969 (2012)
21. D. Kumar, S.A. Hashmi, J. Power Sources **195**, 5101 (2010)
22. X. Qi, Q. Ma, L. Liu, Y.S. Hu, H. Li, Z. Zhou, X. Huang, L. Chen, ChemElectroChem **3**, 1741 (2016)
23. H. Che, S. Chen, Y. Xie, H. Wang, K. Amine, X.Z. Liao, Z.F. Ma, Energy Environ. Sci. **10**, 1075 (2017)
24. A. Arya, A.L. Sharma, J. Mater. Sci. **54**, 7131 (2019)
25. Y. Tominaga, M. Endo, Electrochim. Acta **113**, 361 (2013)
26. W. Liu, S.W. Lee, D. Lin, F. Shi, S. Wang, A.D. Sendek, Y. Cui, Nat. Energy **2**, 1 (2017)
27. M. Ravi, K.K. Kumar, V.M. Mohan, V.V.R.N. Rao, Polym. Test. **33**, 152 (2014)
28. S.A. Suthanthiraraj, B.J. Paul, Ionics (Kiel). **13**, 365 (2007)
29. K.W. Chew, K.W. Tan, Int. J. Electrochem. Sci. **6**, 5792 (2011)
30. D.K. Pradhan, B.K. Samantaray, R.N.P. Choudhary, A.K. Thakur, J. Power Sources **139**, 384 (2005)
31. P.A.R.D. Jayathilaka, M.A.K.L. Dissanayake, I. Albinsson, B.E. Mellander, Electrochim. Acta **47**, 3257 (2002)
32. S.A. Suthanthiraraj, D.J. Sheeba, Ionics (Kiel). **13**, 447 (2007)
33. K. Sundaramahalingam, D. Vanitha, N. Nallamuthu, A. Manikandan, M. Muthuvinayagam, Phys. B Condens. Matter **553**, 120 (2019)
34. L. Bertolla, I. Dlouhý, P. Tatarko, A. Viani, A. Mahajan, Z. Chlup, M.J. Reece, A.R. Boccaccini, J. Eur. Ceram. Soc. **37**, 2727 (2017)
35. P.S. Anantha, K. Hariharan, Solid State Ionics **176**, 155 (2005)
36. B. Liang, S. Tang, Q. Jiang, C. Chen, X. Chen, S. Li, X. Yan, Electrochim. Acta **169**, 334 (2015)
37. S.P. Gejji, C.H. Suresh, K. Babu, S.R. Gadre, J. Phys. Chem. A **103**, 7474 (1999)
38. A.A. Mohamad, N.S. Mohamed, M.Z.A. Yahya, R. Othman, S. Ramesh, Y. Alias, A.K. Arof, Solid State Ionics **156**, 171 (2003)
39. A.R. Polu, R. Kumar, H.W. Rhee, Ionics (Kiel). **21**, 125 (2015)

40. D. Vanitha, S.A. Bahadur, N. Nallamuthu, S. Athimoolam, A. Manikandan, J. Inorg. Organomet. Polym. Mater. **27**, 257 (2017)
41. V. Parameswaran, N. Nallamuthu, P. Devendran, E.R. Nagarajan, A. Manikandan, Phys. B Condens. Matter **515**, 89 (2017)
42. L.P. Teo, M.H. Buraidah, A.F.M. Nor, S.R. Majid, Ionics (Kiel). **18**, 655 (2012)
43. S. Nithya, S. Selvasekarapandian, M. Premalatha, Ionics (Kiel). **23**, 2767 (2017)
44. B.L. Papke, J. Electrochem. Soc. **129**, 1434 (1982)
45. N.M. Zain, A.K. Arof, Mater. Sci. Eng. B **52**, 40 (1998)
46. Z. Shen, G.P. Simon, Y.B. Cheng, Eur. Polym. J. **39**, 1917 (2003)
47. A. Dey, S. Karan, S.K. De, Solid State Commun. **149**, 1282 (2009)
48. A.M. Abo El Ata, S.M. Attia, T.M. Meaz, Solid State Sci. **6**, 61 (2004)
49. D.K. Mahato, A. Dutta, T.P. Sinha, Phys. B Condens. Matter **406**, 2703 (2011)
50. N.A. Hegab, A.E. Bekheet, M.A. Afifi, L.A. Wahab, H.A. Shehata, J. Ovonic Res. **3**, 71 (2007)
51. C.R. Mariappan, G. Govindaraj, Mater. Sci Eng. B Solid-State Mater. Adv. Technol. **94**, 82 (2002)
52. N.A. Hegab, H.M. El-Mallah, Acta Phys. Pol. A **116**, 1048 (2009)
53. A. Arya, A.L. Sharma, J. Mater. Sci. Mater. Electron. **29**, 17903 (2018)
54. S. Chapi, S. Raghu, H. Devendrappa, Ionics (Kiel). **22**, 803 (2016)
55. P. Perumal, S. Selvasekarapandian, K.P. Abhilash, P. Sivaraj, R. Hemalatha, P.C. Selvin, Vacuum **159**, 277 (2019)
56. L. TianKhoon, N. Ataollahi, N.H. Hassan, A. Ahmad, J. Solid State Electrochem. **20**, 203 (2016)
57. D.Y. Zhou, G.Z. Wang, W.S. Li, G.L. Li, C.L. Tan, M.M. Rao, Y.H. Liao, J. Power Sources **184**, 477 (2008)
58. D. Saikia, H.Y. Wu, Y.C. Pan, C.P. Lin, K.P. Huang, K.N. Chen, G.T.K. Fey, H.M. Kao, J. Power Sources **196**, 2826 (2011)
59. C.M. Yang, H.S. Kim, B.K. Na, K.S. Kum, B.W. Cho, J. Power Sources **156**, 574 (2006)